Muller, N., and Birkhahn, R. H. (1968), *J. Phys. Chem. 72*, 538.
Muller, N., and Johnson, T. W. (1969a), *J. Phys. Chem. 73*, 2042.
Muller, N., and Johnson, T. W. (1969b), *J. Phys. Chem. 73*, 2460.
Pallansch, M. J., and Briggs, D. R. (1954), *J. Am. Chem. Soc. 76*, 1396.
Paquette, R. G., Lingafelter, K. C., and Tartar, H. V. (1943), *J. Am. Chem. Soc. 65*, 686.
Pople, J. A., Schneider, W. G., and Bernstein, H. J. (1959), High Resolution Nuclear Magnetic Resonance, New York, N. Y., McGraw-Hill.
Reynolds, J. A., Herbert, S., Polet, H., and Steinhardt, J. (1967), *Biochemistry 6*, 937.
Scatchard, G., Coleman, J. S., and Shen, A. L. (1957), *J. Am. Chem. Soc. 79*, 12.
Spotswood, T. M., Evans, J. M., and Richards, J. H. (1967), *J. Am. Chem. Soc. 89*, 5052.
Sykes, B. D. (1969), *J. Am. Chem. Soc. 91*, 949.
Zeffren, E., and Reaville, R. E. (1968), *Biochem. Biophys. Res. Commun. 32*, 73.

Multioscillator Fluorescence Depolarization. Anisotropy of Dye Binding*

Bernard Witholt† and Ludwig Brand

ABSTRACT: Fluorescence polarization measurements can be used to determine whether dyes bind to proteins with specific or random orientations. Polarization, as a function of temperature and viscosity, is measured at several exciting wavelengths corresponding to various absorption oscillators. In this way there is a photoselection for different protein–dye ensembles whose emission will be observed. A theoretical analysis indicates that it is possible to distinguish a specific orientation of the bound dye relative to the protein, from a random orientation, provided that the protein is not a sphere. Examples of specific as well as random binding have been observed with dyes bound to liver alcohol dehydrogenase and bovine serum albumin. Situations where a dye can rotate independently of the protein are also discussed.

The interaction between small molecules and proteins is usually described in terms of stoichiometry, binding affinity, and the relationships between the various binding sites (Weber, 1965). While such data are basic to an understanding of protein–ligand interactions, additional information about binding can be obtained. For example, it is of interest to obtain an estimate of the extent of orientation of a small molecule relative to a protein. A study of the orientational anisotropy as a function of temperature, pH, or number of moles of a small molecule bound to a protein would complement other binding data to yield an improved picture of the molecular interaction.

One approach for evaluating the orientational anisotropy of bound dyes is that of Weber and Anderson (1969) who examined the energy transfer between several 1-anilinonaphthalene-8-sulfonate molecules bound to bovine serum albumin. They concluded that there is orientational anisotropy in this system, *i.e.*, that the binding is not random. This method requires that more than 1 molecule of dye be bound per protein molecule since otherwise energy transfer will not occur.

This paper describes another approach, based on depolarization of fluorescence at different exciting wavelengths, which allows us to discriminate between random and specific orientation of a single ligand bound to a prolate ellipsoid. Using this method we have compared the extent of orientational specificity of several complexes and conjugates. Only a few of these will be illlustrated here as examples of the applicability of the method.

We also measured the degree of orientational anisotropy, σ, of anilinonaphthalenesulfonate adsorbed to bovine serum albumin as a function of $\bar{n}$, the average number of anilinonaphthalenesulfonate molecules bound per bovine serum albumin molecule.

Theory

Binding Classes. It is convenient to postulate three general binding classes. Class I encompasses those protein–dye adducts in which the dye always maintains a constant orientation relative to the protein axes. The dye absorption and emission oscillators can thus be regarded as intrinsic protein oscillators, uniquely fixed relative to the protein. Class II adducts are those in which the dye is fixed relative to the protein, but in a

* Contribution No. 586 from the McCollum-Pratt Institute, The Johns Hopkins University, Baltimore, Maryland 21218. *Received August 28, 1969.* Supported by Grants No. GM-11632 and 1-F1-GM 36,008 from the National Institutes of Health.

† Portions of the material presented here were taken from a thesis submitted by B. W. to The Johns Hopkins University in partial fulfillment of the requirements for the Ph.D. degree. The present address of Bernard Witholt is The Department of Biochemistry, University of California at San Diego, San Diego, Calif.

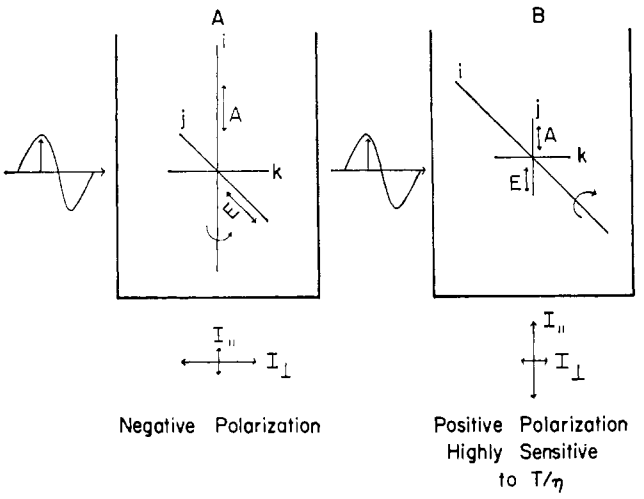

FIGURE 1: Two different oscillator orientations relative to a prolate ellipsoid, illustrating the effect of T/η on the polarization of emission. E = emission oscillator and A = absorption oscillator.

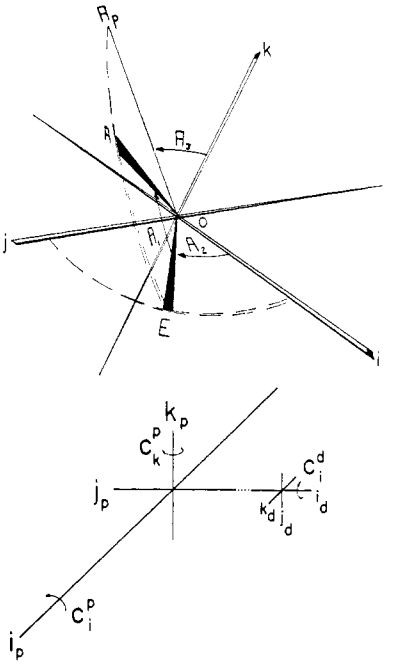

FIGURE 2: Top: oscillator orientations relative to an ellipsoid of revolution around axis i. Axes j and k are identical. E is the emission oscillator in the ij plane, forming an angle A_2 with i. A is the absorption oscillator in the A_pOE plane, forming an angle A_1 with E, while A_p makes an angle A_3 with axis k. A_p is perpendicular to E. Bottom: relationship of a freely rotating chromophore relative to a protein molecule. Subscripts and superscripts p and d refer to the protein and dye, respectively. The chromophore rotates freely about the $j_p = i_d$ axis, limited only by C_i^d, the rotational frictional coefficient around the dye i_d axis. Rotation of the i_d axis, however, depends on ρ_j^p, the protein j axis rotational relaxation time.

random orientation. Class III adducts are those in which the dye is not fixed relative to the protein but rotates independently about a covalent bond.

Classes I–III represent extremes. Experimentally most adducts will probably fall somewhere between these extremes. It will be shown that a detailed analysis of normalized Perrin plots can differentiate between all of these classes. The main purpose of this paper is to show how variations from class II to class I can be determined.

Perrin's Equation for Depolarization of Emission of Ellipsoids of Revolution. Depolarization of fluorescence offers an excellent means of studying the orientational relationship of a fluorochrome relative to a protein. This is so because the absorption and emission oscillators, which are fixed relative to the fluorochrome, rotate with the protein causing depolarization of the emitted light.

If separate absorption dipoles are excited at different wavelengths, differences in the depolarization of emission at each exciting wavelength will depend on the orientation of the dipoles relative to the protein molecule. This can qualitatively be seen in Figure 1, which shows the polarization to be expected due to fluorescence from a dye bound to a prolate ellipsoid of revolution with its emission oscillator parallel to the short axis of the ellipsoid. In Figure 1a the absorption oscillator of the dye is parallel to the long axis of the ellipsoid. In Figure 1b the absorption oscillator of the dye is parallel to the short axis of the ellipsoid. In the first case excitation by vertically polarized light preferentially selects those prolates which have their long axes parallel to the electric vector of the incident beam. These same prolates rotate mainly about their long axis. The emission oscillator will therefore remain in a horizontal plane. Since depolarization depends on randomization of the emission oscillator in the plane normal to the direction of the emitted beam, there will be little depolarization in this case. In contrast, Figure 1b shows the exciting light photoselecting prolates with the long axis perpendicular to the electric vector of the incident beam. This occurs because the absorption dipole for the second exciting wavelength is parallel to the short axis of the prolate ellipsoid. In this case rotation causes a rapid depolarization of the emission (randomization in the plane normal to the emitted beam). It is clear therefore that excitation at several wavelengths produces different amounts of depolarization if the chromophore binds to the protein in an orientationally specific manner. Conversely, variations in the amount of depolarization at various exciting wavelengths can be used as a diagnostic tool to establish orientationally specific (class I) binding.

The situation is quite different in the case of class II binding. Since the fluorochromes are bound with random orientations relative to the axes of the prolate ellipsoid, excitation with vertically polarized light will photoselect a heterogeneous population of ellipsoids whose major axes make all possible orientations with respect to the electric vector of the incident beam. Therefore, no differences in depolarization as a function of wavelength would be expected.

Results are best expressed as normalized Perrin plots plotting U/U_0 as a function of T/η. These terms originate from Perrin's (1926) equation for depolarization of fluorescence of a sphere

$$\frac{U}{U_0} = \frac{\frac{1}{P} - \frac{1}{3}}{\frac{1}{P_0} - \frac{1}{3}} = 1 + \frac{RT}{V_m\eta}\tau = 1 + \frac{3\tau}{\rho_0}$$

TABLE I: Oscillator Orientations and Associated U_0, $P_0°$ for the Various Cases Resulting in the Normalized Perrin Plots Shown in Figure 3.

Case	X	deg A_2	deg A_3	deg A_1	U_0	$P_0°$	Orientation of Emission Dipole	Orientation of Absorption Dipole
a	1						Inconsequential	Inconsequential
b	5	0					Parallel to i axis	Inconsequential
c	5	90		0	1.667	3.000	Parallel to j axis	Parallel to j axis
d	5	90	0	48.19	10	1.214	Parallel to j axis	In jk plane
e	5	90	0	51.42	20	1.103	Parallel to j axis	In jk plane
f	5	90	0	54.06	100	1.020	Parallel to j axis	In jk plane
g	5	90	0	55.41	−100	0.980	Parallel to j axis	In jk plane
h	5	90	0	58.19	−20	0.903	Parallel to j axis	In jk plane
i	5	90	0	61.87	−10	0.812	Parallel to j axis	In jk plane
j	5	90	0	90	−3.33	0.500	Parallel to j axis	Parallel to k axis
k	5	90	90	48.19	10	1.214	Parallel to j axis	In ij plane
l	5	90	90	51.42	20	1.103	Parallel to j axis	In ij plane
m	5	90	90	54.06	100	1.020	Parallel to j axis	In ij plane
n	5	90	90	55.41	−100	0.980	Parallel to j axis	In ij plane
o	5	90	90	58.19	−20	0.903	Parallel to j axis	In ij plane
p	5	90	90	61.87	−10	0.812	Parallel to j axis	In ij plane
q	5	90	90	90	−3.33	0.500	Parallel to j axis	Parallel to i axis

$$P_0° = \frac{I_V}{I_H} \text{ at } \frac{T}{\eta} \rightarrow 0$$

(See Appendix I for definition of terms.) This equation is equally applicable in the case of random binding to ellipsoids of revolution in which case ρ_h is substituted for ρ_0. ρ_h represents the harmonic mean of the individual rotational relaxation times of the ellipsoid axes (Weber, 1952). Finally, in the case of specific binding to prolates, an apparent rotational relaxation time ρ_a can be measured, which may or may not reflect real rotational relaxation times of specific ellipsoid axes.

Models. Perrin's equations (1934, 1936) for the depolarization of emission due to rotation of ellipsoids were used to write a computer program which calculates U/U_0 as a function of T/η for a given ellipsoid dye complex. Perrin's equation was rewritten in terms of the angles and axial ratio, X, shown in Figure 2. The equations necessary to calculate U/U_0 *vs.* T/η are given in Appendix I. No derivations are given; however, results are identical with those of Memming (1961) who rederived Perrin's (1936) equation for the specific case of ellipsoids of revolution using a different set of angles to describe the orientation of the chromophore relative to the ellipsoid.

Table I illustrates a number of specific oscillator orientations relative to a prolate ellipsoid with $X = 5$ and $V_m = 50{,}000$ ml/mole. The dye is assumed to be fixed in the position listed in Table I, and has an excited-state lifetime of 5 nsec. The appropriate normalized Perrin plots for each case are shown in Figure 3.

Note that the molar volume and axial ratio are constant except for case a, which shows the normalized Perrin plot for a sphere of $V_m = 50{,}000$ ml/mole. It is clear, therefore, that the orientation of a dye on a prolate ellipsoid is of crucial importance when depolarization data (*i.e.*, Perrin plots or normalized Perrin plots) are interpreted.

Table I and Figure 3 show only a small number of specific cases, with the emission oscillator parallel to the i or j axis of the ellipsoid. Similar results are obtained at other values of A_2 and A_3. The following generalizations can be made: (1) Unless A_1 is between 50 and 60° (*i.e.*, when P_0 is close to 0) normalized Perrin plots for most ellipsoids will be reasonably straight lines. Curvatures of normalized Perrin plots increase as X increases and P_0 approaches 0. (2) Variations in normalized Perrin plot slopes are large and unless the protein is a sphere, normalized Perrin plots obtained at different exciting wavelengths will be different. This criterion has been used by Steiner and McAlister (1957) and Winkler (1965) to establish the presence or absence of orientational anisotropy.

As an example, case b (emission oscillator parallel to the protein i axis) yields $\rho_i = 285.8$ nsec, while case c (both oscillators parallel to the j axis) yields $\rho_j = 78$ nsec. Since those are in fact the rotational relaxation times of the i and j axes, respectively, for an ellipsoid with $X = 5$ and $V_m = 50{,}000$ ml/mole, it is clear that in these examples the dipole oscillators reflect the rotation of specific protein molecular axes. Thus it is incorrect to measure protein rotational relaxation times on the basis of a Perrin plot if truly random binding has not been demonstrated (Weber, 1953). (3) If all normalized Perrin plots for a protein–dye adduct are identical either the binding of the dye relative to the protein is completely random or the protein approximates a sphere or oblate ellipsoid. Figure 3 is thus the basis for the qualitative arguments presented in the previous section. It illustrates how deviations among normalized Perrin plots obtained at dif-

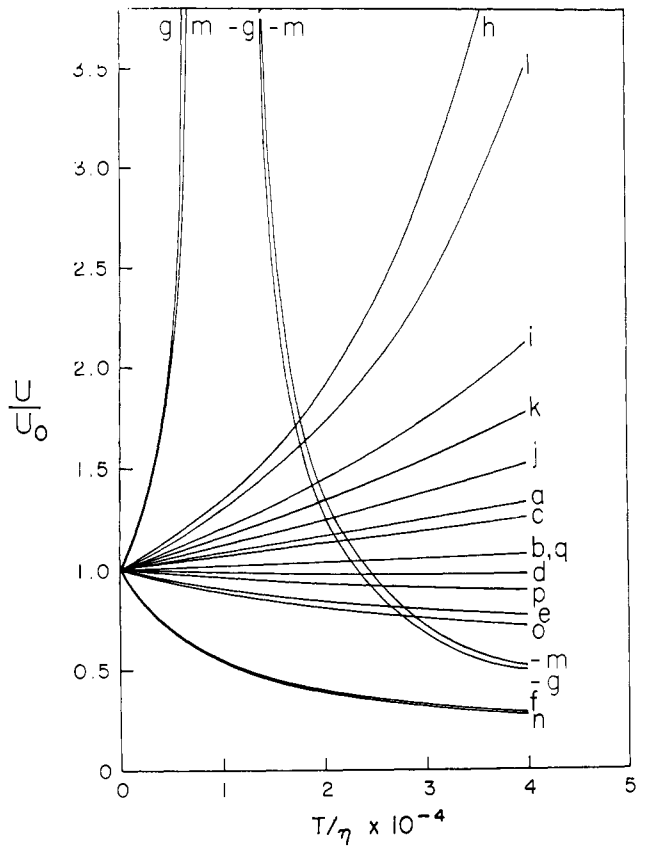

FIGURE 3: Normalized Perrin plots for a sphere (curve a) and a prolate (curves b–q) as generated by a FORTRAN IV program based on the equations in Appendix I. A molecular volume of 50,000 ml/mole is assumed for both prolate and sphere, which have axial ratios of 5 and 1, respectively. The associated chromophore has a lifetime of 5 nsec and the specific oscillator orientations relative to the ellipsoid are listed in Table I. Note that curves g and m disappear toward $+\infty$ and then reappear from $-\infty$. The negative portions of curves g and m have been multiplied by -1 and are plotted as positive curves.

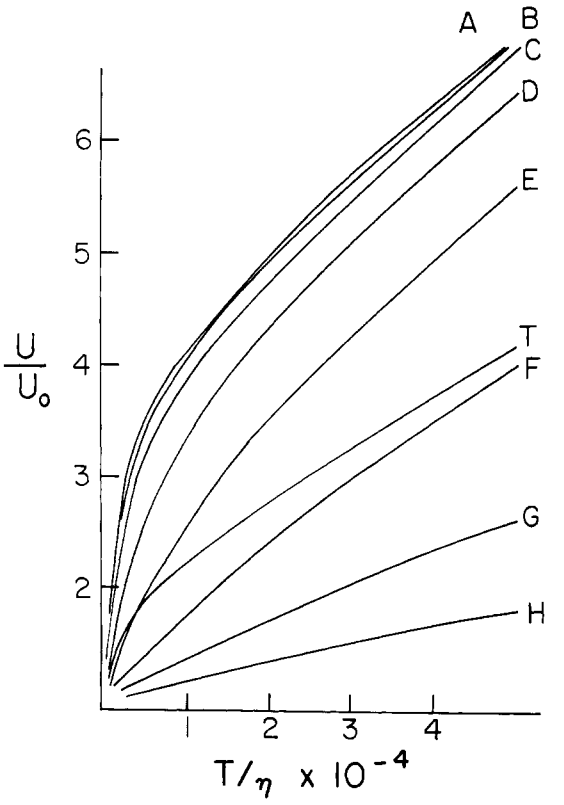

FIGURE 4: Computer generated normalized Perrin plots for a protein–dye system. The amount of dye rotation relative to the protein depends on r, the degree of rigidity between the dye and protein, which varies between $r = 0$ (free rotation) and $r = 1$ (dye is fixed relative to protein). The protein–dye system described is a 200-ml/mole dye molecule coupled to a 50,000-ml/mole sphere. The excited state lifetime of the dye is 10 nsec and the parallel absorption and emission oscillators are normal to the covalent bond between the protein and the dye. The following values of r were used:

Curve	r	Curve	r
A	0	E	0.03
B	0.001	F	0.1
C	0.003	G	0.3
D	0.01	H	1.0

T = The result for a mixture of equivalent amounts of all the above protein dye systems.

ferent exciting wavelengths can be used to assess σ, the degree of orientational anisotropy of binding. (See Appendix II for definition of σ.)

While Figure 3 illustrates normalized Perrin plots to be expected for various cases of class I binding, Figure 4 shows the results for class III binding. This result was predicted by Weber (1952) and Gottlieb and Wahl (1963) who observed these effects. Referring to Figure 2 (bottom), as the rigidity between the protein and dye decreases, the rotation of the dye about i_d (dye i axis) is limited only by C_i^d, the frictional coefficient to rotation of the dye. Rotation about k_p and i_p (protein k and i axes), however, is limited by the frictional coefficients to rotation of the protein about these axes. The resulting normalized Perrin plot reflects the rotational relaxation time of the free dye at very low T/η and the rotational relaxation time of the protein at high T/η. It is clear, therefore, that normalized Perrin plots can be used to distinguish free-dye rotation (class III binding) from a fixed dye configuration (classes I and II binding), although very careful measurements have to be made to distinguish curve F (Figure 4) from any other typical linear normalized Perrin plot. It should be noted that a small amount of free rotation may alter the normalized Perrin plot slope drastically without introducing a measurable curvature. While such partial rotation is to be expected for covalent conjugates, it is not likely to occur in noncovalent adducts since the latter probably depend on many small delocalized forces to effect binding.

Normalized Perrin Plot Analysis. INTERPRETATION OF RESULTS. Differences among normalized Perrin plots obtained at different exciting wavelengths rest on differences in the rotational relaxation times of each of the three axes of the postulated ellipsoid. It can thus be expected that the sensitivity of such an analysis will increase as the differences in the various axial lengths increase. While Perrin's equation for ellipsoids of revolution was used, the situation is more complex in nature since most proteins are probably more closely approximated by ellipsoids with three unequal axes.

A qualitative diagnosis of experimental data is suggested in the right-hand column of Table II, which may be used by

TABLE II: Interpretations of Normalized Perrin Plot Configurations.

Normalized Perrin Plot Slope Variation as T/η Increases	Relationship between Normalized Perrin Plots at Different λ_{ex}	Other Variables	Diagnosis
Decreases rapidly	Identical		Mixture of two or more components: size differential increases as curvature of normalized Perrin plots increases. May be due to free dye fluorescence or formation of dimers, tetramers, or aggregation.
	Nonidentical		Dye rotation (either dye itself or adjoining protein segment) relative to bulk of the protein.
Invariant	Identical	$\rho_h/\rho_0 < 2$	Random binding to any ellipsoid or specific binding to oblates.
		$\rho_h/\rho_0 > 2$	Oblate, or an error in the estimate of ρ_0.
		Similar results for several dyes	Must be an oblate. Calculate X from ρ_h/ρ_0.
	Nonidentical		Prolate

fitting the normalized Perrin plots to be examined in one of the categories listed in the three leftmost columns.

Experimental Procedures

Materials. The dyes used in this work were 1-anilinonaphthalene-8-sulfonate and 2-anthracene isocyanate. Anilinonaphthalenesulfonate was crystallized as described by Turner and Brand (1968). Anthracene isocyanate was prepared from 2-aminoanthracene (K & K Laboratories, Inc., Plainview, N. J.) using the procedure of Fieser and Creech (1939). The isocyanate was recrystallized from benzene.

Crystalline bovine serum albumin (lot no. D71209) was obtained from the Armour Pharmaceutical Co. (Chicago, Ill.).

Horse liver alcohol dehydrogenase (EC 1.1.1.1) was obtained from the Boehringer Mannheim Corp. (New York, N. Y.) as a crystalline suspension, and dialyzed for 24 hr against 0.1 M sodium phosphate (pH 7.4) at 4°.

Bovine serum albumin–anthracene and horse liver alcohol dehydrogenase–anthracene were made by conjugating anthracene isocyanate (in dioxane) with bovine serum albumin or horse liver alcohol dehydrogenase in 0.1 M carbonate–bicarbonate (pH 9.3). Unreacted dye was removed by eluting the conjugate from a Sephadex G-25 fine column (Pharmacia Chemicals, Inc., Uppsala, Sweden). The conjugate compositions in mole of dye per mole of protein were less than 1.3, and 3, respectively, assuming that all the dye had been bound to protein.

Bovine serum albumin–anilinonaphthalenesulfonate complex compositions were calculated assuming five binding sites for anilinonaphthalenesulfonate on bovine serum albumin and $K_D = 1.5 \times 10^{-6}$ (Daniel and Weber, 1966).

Analyzed Reagent grade *d*-sucrose was obtained from the J. T. Baker Chemical Co. (Phillipsburg, N. J.). Ultra Pure, density gradient *d*-sucrose was obtained from the Mann Research Laboratories (New York, N. Y.). Mann *d*-sucrose is preferable for this work, since it contains fewer absorbing and fluorescing impurities.

Fluorescent Measurements. All measurements were performed on an instrument described by Witholt and Brand (1968). Perrin plots were obtained by varying T/η, maintaining different sucrose solutions at 20.0°. The exciting band width was as small as possible, compatible with intensity requirements, while the emission band width was almost always 33 mμ for these experiments.

Raw polarization data were corrected for discriminator errors (Witholt and Brand, 1968; Witholt, 1969), and for errors caused by the rotation of the polarized exciting and emitted beam by concentrated sucrose solutions (Witholt, 1969). These corrections never changed the observed degree of polarization by more than 5%. While the absolute precision of such data is of the order of ±2%, the relative accuracy of a set of polarization values obtained under constant discrimination conditions is ±0.2%.

Results

Representative Normalized Perrin Plots for Each of the Various Binding Classes. Figure 5 shows normalized Perrin plots for a covalent bovine serum albumin–anthracene conjugate, which appears to be an example of class I binding. Specific binding of anthracene to bovine serum albumin is suggested by the nonsuperposition of the normalized Perrin plots (compare with Figure 3 and Table II). The curves obtained by excitation at 265 and 280 mμ are equivocal since the intrinsic chromophores of the protein absorb in this region.

Figure 6 shows normalized Perrin plots for horse liver alcohol dehydrogenase–anthracene. Similar results were obtained with horse liver alcohol dehydrogenase–fluorescein (not shown here). There is a marked concave curvature in

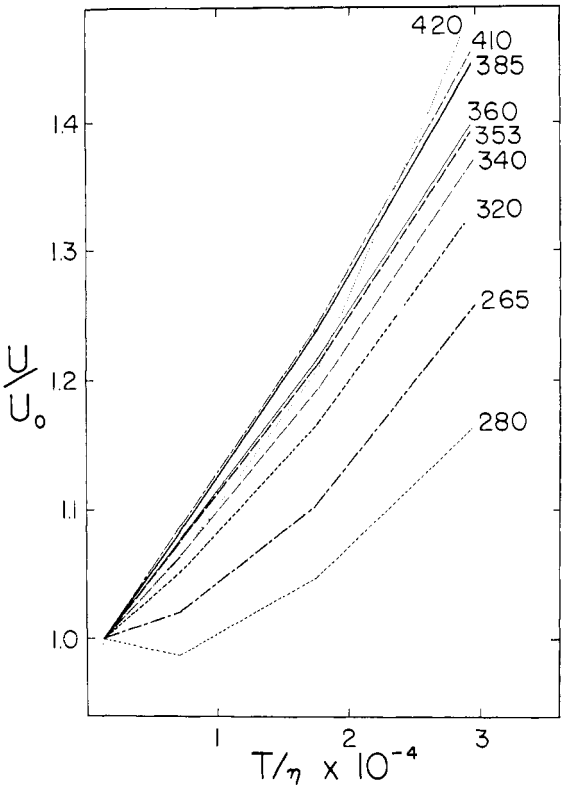

FIGURE 5: Normalized Perrin plots for a bovine serum albumin–anthracene conjugate. The dye to protein ratio was less than 1.3 and the concentration of conjugate was 8.7 μM in 0.1 M Tris (pH 7.3) at 20.0 ± 0.2°. Data were obtained at four sucrose concentrations equivalent to T/η = 1355, 7118, 17,566, and 29,260°K per P (poise). The excitation band width was 4.8 mμ and the emission band width was 33 mμ. The emission monochromator was set at 450 mμ. The excitation wavelength is indicated for each curve.

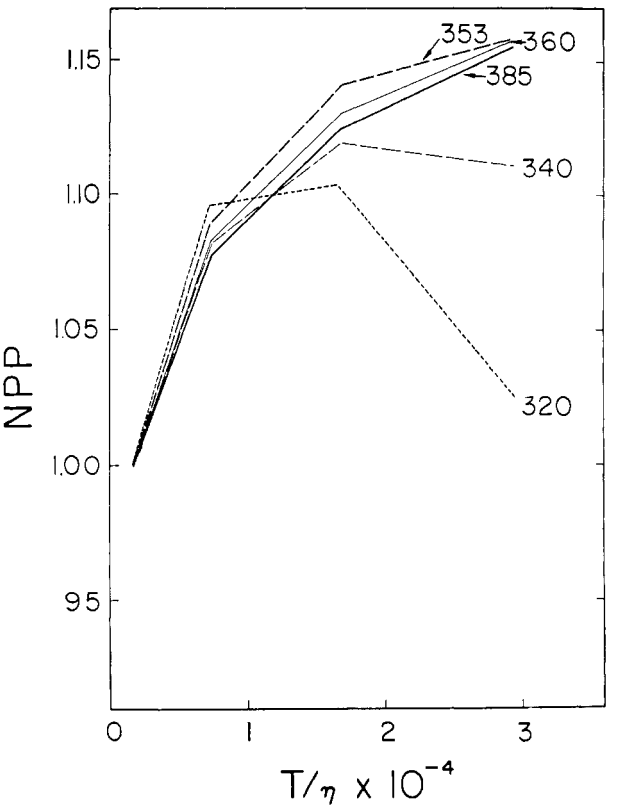

FIGURE 6: Normalized Perrin plots for a horse liver alcohol dehydrogenase anthracene conjugate. The dye to protein ratio was less than 3 and the concentration of conjugate was 10 μM in 0.1 M Tris (pH 7.5) at 20.0 ± 0.2°. Data were obtained at four sucrose concentrations equivalent to 1518, 7377, 16,622, and 29,260°K per P. The excitation band width was 4.8 mμ at the excitation wavelengths indicated for each curve. The emission monochromator was set at 450 mμ.

all of these normalized Perrin plots, suggesting some independent rotational freedom of the dyes relative to the protein. These conjugates are thus examples of class III binding. The low depolarization at high T/η may suggest significant aggregation of the horse liver alcohol dehydrogenase molecules under these conditions.

Figure 7 shows normalized Perrin plots for a bovine serum albumin–anilinonaphthalenesulfonate complex of $\bar{n}$ = 0.64, where $\bar{n}$ is the average number of anilinonaphthalenesulfonate molecules bound per bovine serum albumin molecule. Deviations between the normalized Perrin plots are exceedingly small, suggesting that this complex is an example of class II binding, that is, anilinonaphthalenesulfonate is bound in an orientationally random manner to bovine serum albumin.

Further Analysis of the Bovine Serum Albumin–Anilinonaphthalenesulfonate Complex. The data shown in Figure 7 were obtained by varying the viscosity of a solution of 1.5×10^{-5} M bovine serum albumin and 1.0×10^{-5} M 1,8-anilinonaphthalenesulfonate ($\bar{n}$ = 0.64) in 0.05 M carbonate–bicarbonate buffer. The viscosity was changed by the addition of sucrose which altered the pH from 8.6 to 9.3. The same results were obtained by varying the temperature of 0.1 M sodium phosphate (pH 7.4) containing 1.5×10^{-4} M bovine serum albumin and 1.0×10^{-5} M anilinonaphthalenesulfonate ($\bar{n}$ = 0.067). Thus, increasing [bovine serum albumin] tenfold, changing the buffer composition and pH, and varying either the viscosity or the temperature does not seem to alter the fact that at low $\bar{n}$, the bovine serum albumin–anilinonaphthalenesulfonate complex is a class II complex.

At higher $\bar{n}$, however, increasing deviations among normalized Perrin plots are found, as shown in Figure 8. Normalized Perrin plots for bovine serum albumin–anilinonaphthalenesulfonate are given at $\bar{n}$ = 4.55 (set a) and $\bar{n}$ = 1.93 (set b). These data suggest a transition from class II to class I binding. To quantitate this transition, we calculate σ, the degree of orientational anisotropy, which is a function of the deviations among normalized Perrin plots obtained at different exciting wavelengths. Thus, σ = 0 when the binding is completely random, and σ increases as the binding orientation becomes more specific. σ is defined in Appendix II. Figure 9 shows σ as a function of $\bar{n}$ for bovine serum albumin–anilinonaphthalenesulfonate complexes obtained under the conditions of Figure 8.

It appears that $\sigma = 3 \times 10^{-11}$ is a lower limit, imposed by the uncertainties of the measurement itself. Increases in σ at $\bar{n}$ less than 1 are attributed to experimental error due to the low fluorescence intensity. Increases in σ from $\bar{n}$ = 2 to $\bar{n}$ = 4.5 cannot be explained on that basis, since the signal:noise ratio increases as $\bar{n}$ increases.

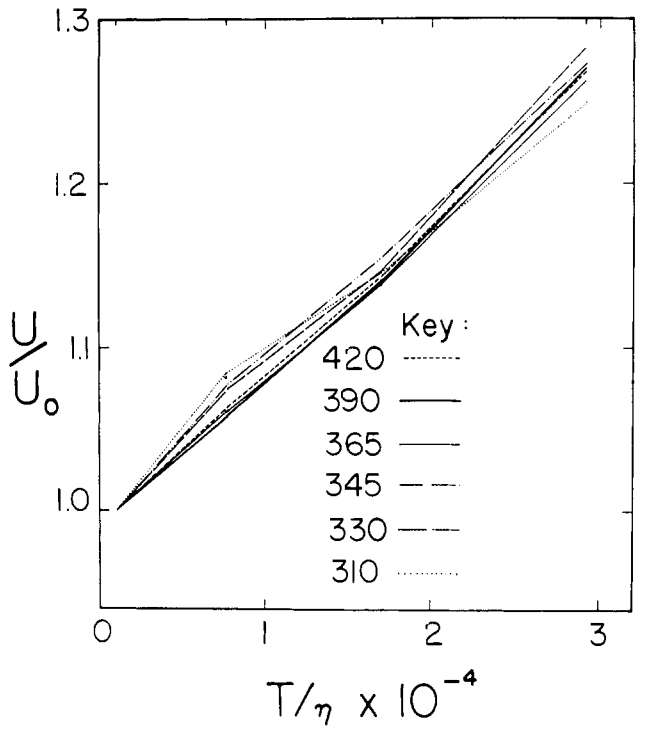

FIGURE 7: Normalized Perrin plots for a 15 μM bovine serum albumin–anilinonaphthalenesulfonate complex. The protein had 0.64 mole of dye adsorbed per mole of protein. The solvent was 0.05 M carbonate–bicarbonate buffer at pH 9.0 at 20.0 ± 0.2°. Data were obtained at four sucrose concentrations equivalent to T/η = 1000, 7672, 16,990, and 29,260°K per P. The excitation band width was 4.8 mμ at the wavelengths indicated for each curve. The emission monochromator was set at 480 mμ.

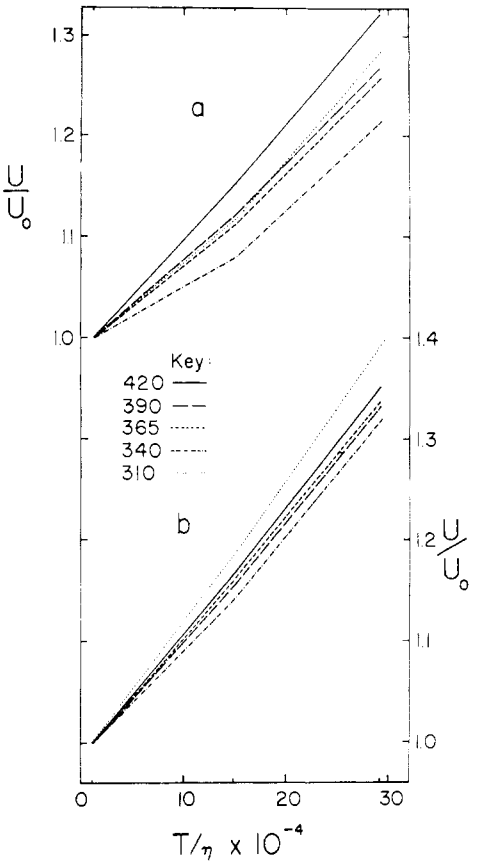

FIGURE 8: Normalized Perrin plots for two bovine serum albumin–anilinonaphthalenesulfonate complexes. The solvent was 0.1 M sodium phosphate (pH 6.8) at 20.0 ± 0.3°. The excitation band width was 4.8 mμ at the excitation wavelengths indicated for each curve. The emission monochromator was set at 480 mμ. Data were obtained at three sucrose concentrations. For set a, $\bar{n}$ = 4.55 and T/η = 1142, 14,970, and 29,260°K per P; for set b, $\bar{n}$ = 1.93 and T/η = 1087, 14,870, and 29,260°K per P.

Discussion

The data presented in Figures 5–7 demonstrate that it is possible to discriminate among different protein–dye binding classes on the basis of normalized Perrin plots. Figures 8 and 9 suggest the possibility of monitoring orientational specificity as a function of saturation.

Effects of Energy Transfer. When several ligands bind to a protein in a preferential orientation, energy transfer among them may cause changes in the apparent rotational relaxation time, as shown by Weber and Anderson (1969). The apparent rotational relaxation time varies as a function of the amount of energy transfer and the spatial distribution of the oscillators involved. The spatial distribution of the absorption oscillators with respect to the protein changes as a function of exciting wavelength unless the chromophores are oriented randomly. It follows therefore that randomization of the emitted light due to energy transfer does not affect the results obtained for class II binding from normalized Perrin plot analysis. The value of σ for class I, however, may be dependent on energy transfer. Anderson and Weber (1969) have shown that the efficiency of energy transfer among anilinonaphthalenesulfonate molecules bound to bovine serum albumin varies with exciting wavelengths. In practice then, energy transfer among several ligands somewhat obscures the extent of binding specificity as measured by this method, but it still allows a qualitative distinction between specific and random binding to be made.

Anilinonaphthalenesulfonate Binding to Bovine Serum Albumin. Anderson and Weber (1969) have concluded that anilinonaphthalenesulfonate binds bovine serum albumin preferentially in planes parallel to the ellipsoid equator, that is, parallel to the *jk* plane. Our data (Figure 9) indicate that while there appears to be orientational specificity when several anilinonaphthalenesulfonate molecules are bound to bovine serum albumin, there is a decrease in this specificity at low $\bar{n}$.

Potentials and Limitations. The interpretation of the normalized Perrin plots of Figures 5–7 assumes that the lifetime of the excited state is invariant as a function of exciting wavelength, and sucrose concentration. The first assumption is essential, since variations in τ at different exciting wavelengths would affect the normalized Perrin plot slopes. In fact, theory predicts and measurements show that the quantum yield of several substituted naphthalenes is constant at exciting wavelengths above 260 mμ (Witholt, 1969). The second assumption is not essential, since only the curvature of the normalized Perrin plot changes when τ varies with the solution conditions. The relationship between the normalized Perrin plots does not change unless τ varies differently at each exciting wavelength. Therefore, σ is not

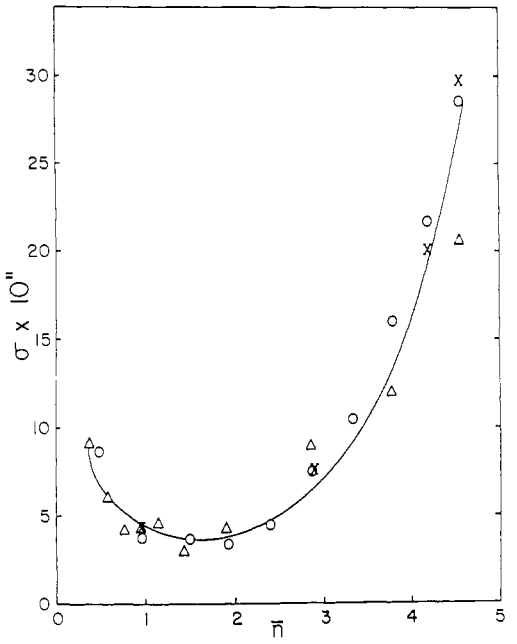

FIGURE 9: Change of σ, the degree of orientational anisotropy with $\bar{n}$. Titration of 50 μM bovine serum albumin with 1,8-anilinonaphthalenesulfonate in 0.1 M sodium phosphate (pH 6.8) at 20.0 ± 0.2°. Each point on this figure is based on a set of normalized Perrin plots such as those shown in Figure 8. $\bar{n}$ was varied by adding 5-μl increments of 1,8-anilinonaphthalenesulfonate. The circles and triangles represent duplicate experiments carried out under slightly different optical conditions. The crosses are exact duplicates of the corresponding circles.

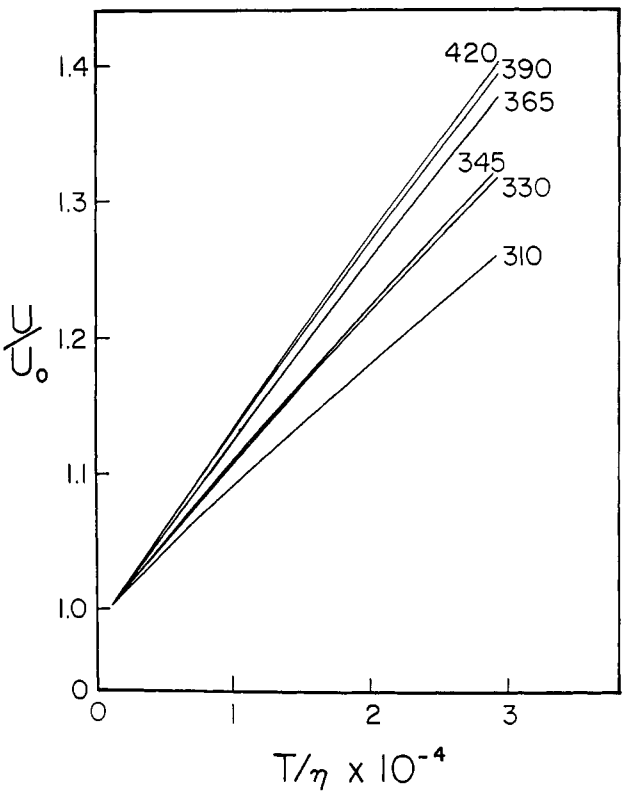

FIGURE 10: Theoretical normalized Perrin plots for a bovine serum albumin–anilinonaphthalenesulfonate complex with one molecule of anilinonaphthalenesulfonate per mole of bovine serum albumin. The calculations were based on the following assumptions. The anilinonaphthalenesulfonate oscillators are all in the *jk* plane of a prolate ellipsoid with $X = 4$ and $V_M = 70{,}000$ ml/mole. Anilinonaphthalenesulfonate has a lifetime of 16 nsec and U_0 and A_1 have the following values at each wavelength.

λ_{ex}	U_0	A_1 (deg)
420	1.977	17.92
390	2.130	21.63
365	2.414	26.46
345	3.337	34.99
330	3.422	35.50
310	4.518	40.27

affected by variations in τ with sucrose concentration since σ only depends on the relationships among the various normalized Perrin plots. The linear normalized Perrin plots of Figure 7 and the fact that similar results are obtained when the temperature rather than sucrose concentration is varied, imply that in this case variations in τ do not occur as a function of sucrose concentration.

A second possible limitation of normalized Perrin plot analysis relates to the relative orientation of the absorption oscillators of the dye. Figure 10 shows normalized Perrin plots for a bovine serum albumin–anilinonaphthalenesulfonate complex assuming an equatorial orientation of the anilinonaphthalenesulfonate plane relative to a prolate ellipsoid of axial ratio $X = 4$ and $V_M = 70{,}000$ ml/mole. That is, anilinonaphthalenesulfonate is parallel to the *jk* plane (Figure 2), has a lifetime of 16 nsec as measured by Anderson and Weber (1969), and has the general dimensions and 40% hydration determined by Squire *et al.* (1968). As can be seen from Figure 10, there are only three groups of normalized Perrin plots, those around 310, 340, and 380 mμ, related to three separate transitions of anilinonaphthalenesulfonate. The rather small deviations between these groups is due to the small differences in A_1, the angle between the different absorption oscillators and the emission oscillator. Better results with such studies can therefore be obtained with dyes which have several positive and negative polarizations, such as rhodamine B or rose bengal. However, differences between Figures 7 and 10 are still sufficient to rule out binding of anilinonaphthalenesulfonate in the *jk* plane of bovine serum albumin when only one mole of anilinonaphthalenesulfonate is bound to bovine serum albumin.

Finally, by directly following the horizontally and vertically polarized components of the emission during the decay time, depolarization can be measured as a function of time (Stryer, 1968). By doing this at different exciting wavelengths, the binding randomness can be assessed without changing the temperature or adding sucrose.

Acknowledgments

The authors are grateful to Professor A. Nason for permission to use his Cary 14 spectrophotometer. Professor R. Ballentine provided useful advice in the synthesis of isocyanates and Professor W. H. Huggins was kind enough to discuss computer techniques with us. We thank Professor W. F. Harrington for valuable discussions and James R. Gohlke who critically read the manuscript.

Appendix I

Perrin's equation for depolarization due to rotation of ellipsoids (eq 53, 56, 58, 59 of Perrin, 1936) was rewritten in terms of the parameters indicated in Figure 2, to facilitate its use in computer programs. From Perrin's eq 56 (1936), and assuming ellipsoids of revolution (*i.e.*, j axis = k axis), and for excitation with vertically polarized light

$$U = \frac{1}{P} - \frac{1}{3} = \frac{2(P^\circ + 2)}{3(P^\circ - 1)} = \frac{5}{3}\frac{K}{[\mathrm{G} + \mathrm{E} - \mathrm{H}]} \quad (1)$$

where

$$\mathrm{P} = \frac{I_\mathrm{V} - I_\mathrm{H}}{I_\mathrm{V} + I_\mathrm{H}}, \; P^\circ = \frac{I_\mathrm{V}}{I_\mathrm{H}} \quad (2)$$

I_V = intensity of vertically polarized emission and I_H = intensity of horizontally polarized emission.

Terms on the right-hand side of eq 1 reflect the rotational relaxation times of the ellipsoid, the orientation of the absorption and emission dipoles relative to the ellipsoid, or both.

From Perrin's eq 58, 59, 53, 10, and 30 (1936)

$$K = (1 + 6B)[1 + 2B(2y + 1)] \quad (3)$$

$$E = 2(y + 2)BG + (y - 1)BF \quad (4)$$

$$H = \frac{9D(y - 1)^2B^2}{1 + (5 + y)B} \quad (5)$$

Based on the angles A_1, A_2, and A_3 defined with respect to Figure 2, the orientational parameters are as follows

$$F = 3[C_1^2C_2^2 - S_1S_2S_3C_1C_2 + S_1^2S_2^2C_3^2] - 1 \quad (6)$$

$$G = 1.5C_1^2 - 0.5 \quad (7)$$

$$D = [C_1^2 - S_1^2S_3^2]S_2^2C_2^2 + S_1S_2S_3C_1C_2(C_2^2 - S_2^2) \quad (8)$$

where

$$C_\mathrm{m} = \cos A_\mathrm{m} \text{ and } S_\mathrm{m} = \sin A_\mathrm{m}$$

B and y are functions of the ellipsoid rotational frictional coefficients and can be derived from eq 9 and 10 of Perrin (1934). Assuming the dye is fixed relative to the protein (class I binding)

$$y = \left(x - \frac{\mathrm{I}}{\gamma}\right)\alpha \quad (9)$$

$$B = \frac{RT\tau}{4V_\mathrm{m}\eta(X^2 - 1)\alpha} \quad (10)$$

where

$$\alpha = \frac{X^2 + 1}{(2X^2 - 1)\frac{\mathrm{I}}{\gamma} - X} \quad (11)$$

$$\gamma = |X^2 - 1|^{1/2} \quad (12)$$

and

$$I = \ln(X + \gamma) \text{ for } X > 1$$
$$I = \arctan(\gamma/X) \text{ for } X < 1 \quad (13)$$

where R = gas constant (8.317×10^7 ergs $^\circ\mathrm{K}^{-1}\,\mathrm{mole}^{-1}$), T = temperature in °K, τ = dye lifetime in seconds, X = axial ratio of the ellipsoid, V_m = prolate molar volume in milliliters per mole, η = solvent viscosity in poises.

Appendix II

Calculation of σ

$$\sigma = \frac{1}{N}\sum_i\sum_j\left[\frac{a_i^j - b_{\mathrm{LE}}^j}{b_{\mathrm{LE}}^j - 1}\frac{1}{\Delta T/\eta]_j}\right]^2 \quad (14)$$

where a_i^j = point on ith normalized Perrin plot, at $\lambda_{ex} = i$ and $T/\eta = j$; b_{LE}^j = point on normalized Perrin plot, where λ_{ex} corresponds to the lowest energy (LE) transition, at $T/\eta = j$; $\Delta T/\eta]_j$ = the difference between $T/\eta]_j$ and $T/\eta]_0$, the lowest value of T/η. N = number of a_i^j points included in the calculation. This definition of σ is needed to make it independent of T and η (hence the term $1/\Delta T/\eta$) and τ (which accounts for the fraction $(a_i^j - b_{\mathrm{LE}}^j)/(b_{\mathrm{LE}}^j - 1)$).

References

Anderson, S. R., and Weber, G. (1969), *Biochemistry 8*, 371.
Daniel, E., and Weber, G. (1966), *Biochemistry 5*, 1893.
Feiser, L. F., and Creech, H. J. (1939), *J. Am. Chem. Soc. 61*, 3502.
Gottlieb, Y. Y., and Wahl, P. (1963), *J. Chem. Phys. 60*, 849.
Memming, R. (1961), *Z. Physik. Chem. (Frankfurt) 28*, 168.
Perrin, F. (1926), *J. Phys. Radium 7*, 390.
Perrin, F. (1934), *J. Phys. Radium 5*, 497.
Perrin, F. (1936), *J. Phys. Radium 7*, 1.
Squire, P. G., Moser, P., and O'Konski, C. T. (1968), *Biochemistry 7*, 4261.
Steiner, R. F., and McAlister, A. J. (1957), *J. Polymer Sci. 24*, 105.
Stryer, L. (1968), *Science 162*, 56.
Turner, D. C., and Brand, L. (1968), *Biochemistry 7*, 3381.
Weber, G. (1952), *Biochem. J. 51*, 145.
Weber, G. (1953), *Advan. Protein Chem. 8*, 415.
Weber, G. (1965), *in* Molecular Biophysics, Pullman, B., and Weissbluth, M., Ed., New York, N. Y., Academic, p 359.
Weber, G., and Anderson, S. R. (1969), *Biochemistry 8*, 361.
Winkler, M. H. (1965), *Biochim. Biophys. Acta 102*, 459.
Witholt, B. (1969), Ph.D. Thesis, Johns Hopkins University, University Microfilms No. 69-13,500.
Witholt, B., and Brand, L. (1968), *Rev. Sci. Instr. 39*, 1271.